

ExoBoot, a soft inflatable robotic boot to assist ankle during walking: Design, Characterization and Preliminary tests

Jinwon Chung*, Roman Heimgartner*, Ciarán T. O'Neill, Nathan S. Phipps and Conor J. Walsh,
Member, IEEE

Abstract— In this paper, we present the design and characterization of the ExoBoot, a soft inflatable robotic boot for assisting ankle plantarflexion during walking. The ExoBoot integrates a soft textile-based actuator and an IMU sensor into a textile boot, making it low-profile and lightweight. The inflatable actuator generates assistive plantarflexion torque when pressurized by bending on top of the boot. We characterize the torque generated by the ExoBoot at various pressures and ankle angles, achieving a maximum torque of 39 Nm at 483 kPa (70 psi) and 60 degrees ankle angle. In order to evaluate the performance of the ExoBoot during walking, a pilot study with one healthy subject was conducted. Actuation is triggered by an open loop pressure controller, based on the ankle angular velocity measured by an IMU, using high flow rate solenoid valves. At the peak of active assistance, pressure in the actuator reaches 75% of the supply pressure, and maximum torque applied on the ankle is estimated to be 23 Nm. These results demonstrate potential for the ExoBoot to reduce the metabolic cost of walking.

I. INTRODUCTION

A number of lower-extremity wearable robots have been developed to assist or augment human walking, their applications ranging from functional assistance or rehabilitation [1], [2] to endurance or performance augmentation [3]–[6]. Rigid structures have traditionally been levered to directly transfer load to the ground and deliver high torques to the joints [7], [8]. However, despite enabling higher levels of assistance, rigid exoskeletons are challenging to align with the biological joints, restrict the wearer's natural movements and apply undesired forces when misaligned [9]. Additionally, these structures add inertia to the limbs, increasing the metabolic cost of locomotion for healthy individuals [10].

Recently, there is a trend to more lightweight and simple systems that are comfortable to wear for extended periods of time. This approach uses low-profile components anchored to the body to transmit tensile forces to the limbs, some components being rigid [4], [5], [11] and some being compliant such as the soft exosuit [2], [6], [12]. The exosuit is a cable-driven system that transmits forces to functional

This material is based upon work supported by the Office of Naval Research (ONR) award number N00014-17-1-2121, the Wyss Institute for Biologically Inspired Engineering and the John A. Paulson School of Engineering and Applied Sciences at Harvard University.

* These authors equally contribute to this work.

J. Chung (e-mail: jinwonchung@seas.harvard.edu), R. Heimgartner (e-mail: roman_heimgartner@gmail.com) and C. Walsh (phone: 617-496-7128, e-mail: walsh@seas.harvard.edu) are with the John A. Paulson School of Engineering and Applied Sciences and the Wyss Institute for Biologically Inspired Engineering, Harvard University, Cambridge, MA 02138 USA

textiles anchored to the limbs. Cable transmission allows the heavier components to be worn on a more proximal body location such as the waist so that added inertia to the body can be minimized. However, this approach, when combined with interfacing to the body via functional apparel anchors, presents technical challenges in delivering comfortable and controlled assistance to the wearer.

Another approach explored by some groups for the development of lightweight wearable robots is the use of pneumatic or fluid-powered systems. This approach also enables power to be transmitted remotely so that components on the limb can be lightweight. One of the most common types of pneumatic actuator used in wearable robots is the McKibben actuator, which contracts when inflated and display force-length properties similar to those of skeletal muscles [11], [13], [14]. McKibben actuators are both compliant and able to generate large force, but a major caveat comes from their limited stroke length. Thus, when attached across a joint, these actuators can place constraints on the user's natural motion.

Recent developments have led to alternatives to McKibben actuators which can extend, bend, twist and combinations thereof [15]–[17]. These types of actuators were investigated for upper extremity assistive devices, capitalizing upon the anisotropic properties of fabrics and elastomers [15], [18]. The advent of these new actuators has enabled the

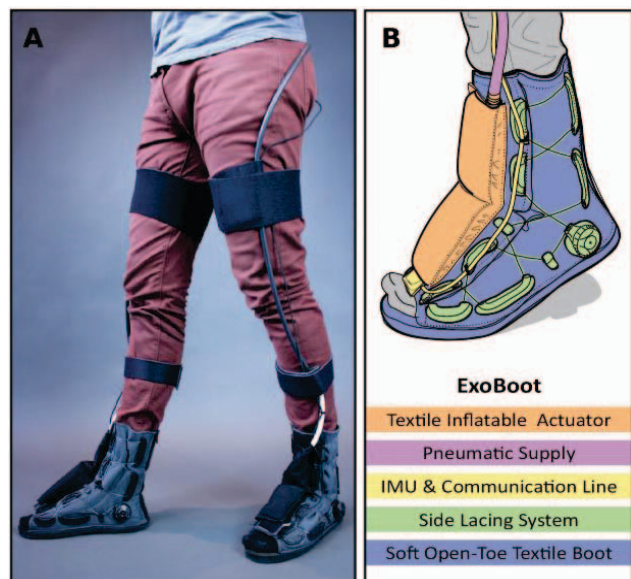


Figure 1 A. Picture of the ExoBoot worn by a human. B. Diagram of ExoBoot with components labeled

development of compact devices for hand rehabilitation [19] and devices that provide high torque for shoulder assistance [20]. Recently, these alternative inflatable actuators have begun to be applied to lower extremity wearable devices as well. Sovero et al. introduces an ankle assistance device using soft and rigid components that is capable of generating high torques [16] and Sridar et al. describes a compact and soft knee rehabilitation device [17]. In this paper, we focus on ankle assistance, as the ankle is responsible for generating about 45% of the power during gait [21]. We argue that for wearable ankle assistive robots to be most effective, they must: (i) be soft and lightweight, (ii) have a compact and integrated design and (iii) provide high torques. These characteristics minimize inhibition of the user's natural gait, while maximizing the assistance.

We present ExoBoot, a soft, inflatable robotic boot that integrates the actuation, sensing and human-robot interface elements, while being capable of generating significant torque at a normal walking pace. The ExoBoot consists of a custom-made textile boot, a textile-based inflatable actuator and an IMU sensor. It is designed to assist ankle plantarflexion in the sagittal plane and not to restrict other ankle motions. At first, we aimed to assist healthy subjects to verify its feasibility. In this paper, we detail the design of the integrated boot, the control hardware and an initial algorithm for delivering assistance during walking. We provide actuator characterization on an instrumented ankle rig to understand the relationship between generated torque, supply pressure and ankle angle. We describe the control strategy to assist ankle plantarflexion during walking and a dynamic torque estimation method using data from static actuation characterization. Finally, we present results from preliminary testing on a healthy subject to show that the device can deliver a sufficient amount of assistance during walking.

II. A SOFT INFLATABLE ROBOTIC BOOT FOR ANKLE ASSISTANCE

A. Preliminary design considerations

Maximum assistive torque generated by soft wearable robots is generally much smaller compared to that of rigid exoskeletons [22]. Therefore, preliminary insights in terms of assistive torque profile needs are crucial to guide and validate the design of a low-profile soft pneumatic ankle device that assists walking at comfortable speeds (1 - 1.5 m/s). We aim at providing similar levels of peak torque (20 Nm to 50 Nm) compared to other soft ankle exoskeletons [5], [6], [23]. Knowing that a linear model well describes the relationship between the peak ankle assistive torque of the cable-driven exosuit and the net metabolic reduction [6], our device could still demonstrate promising results by delivering as low as 20 Nm.

The assistive torque on the ankle joint must be applied synergistically with the underlying plantarflexor muscles. They typically activate at the beginning of stance and peak at approximately 50% of the gait cycle (GC).

The actuation must therefore be timed correctly to satisfy this requirement. From literature, it appears that a torque

onset timing of 30 - 35% GC and an off timing of 60 - 65% GC fit well in the range observed for most subjects. Moreover, peak timing most often lies at approximately 50% GC. Even though optimal actuation timings vary across different subjects, devices and actuation schemes, past studies provide good estimations of what optimal torque onset, peak and off timings could be [24].

The control hardware needs to provide the required pressure in a timely manner to operate the boot at normal walking speeds (1 to 1.5 m/s) which correspond to 45 to 60 strides/min [25]. Recalling the operating range in terms of the gait cycle percentage mentioned before, this implies that actuator should inflate in less than 250 ms and deflate in less than 150 ms.

B. Design overview

The ExoBoot is designed to assist ankle plantarflexion. To generate assistive torques, a cylindrical textile-based inflatable actuator is sewn on top of a flexible custom-made boot. Fig. 2 shows a simplified diagram of the forces applied on the foot and the actuator when supplied with compressed air.

We model the foot and shank as independent rigid bodies linked by a revolute joint as shown in Fig. 2A. Half of the actuator is affixed to the shank and the other half is affixed to the foot. If we assume the shank is fixed, then the forces applied on the foot and the bottom half of the actuator are: the reaction force on the revolute joint F_{joint} , the force induced by air pressure F_{air} , and the sum of tensile forces on the fabric enclosure ΣF_{fabric} .

The actuator exerts torque until it is fully straightened because F_{air} is bigger than ΣF_{fabric} . At the neutral position, the ankle angle is about 90 degrees, as shown in Fig. 2B, and a wrinkle is formed on the anterior side of the fabric enclosure. Due to this wrinkle, it cannot resist tension, and the net tensile force on the enclosure is smaller than F_{air} . Thus, there is a resultant torque that is applied on the foot-actuator system around the ankle joint. At the fully extended position, the actuator and foot are aligned, as shown in Fig. 2C, and

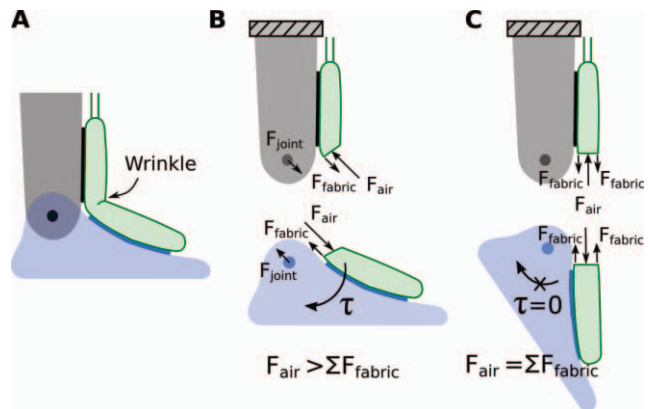


Figure 2 Actuation principle A. Simplified diagram of the actuator-ankle system. It is assumed that the actuator is tightly fixed to the foot and the shank. B. Free body diagram at a 90 degrees ankle angle. The actuator exerts torque to the foot because the fabric enclosure cannot resist tension due to wrinkling, so that ΣF_{fabric} is smaller than F_{air} . C. Free body diagram when the actuator is fully straightened. The actuator cannot apply torque to the foot because ΣF_{fabric} is same as F_{air} due to absence of wrinkle.

the sum of tensile forces on the enclosure exactly balances F_{air} . In this equilibrium configuration, the air pressure no longer generates torque around the ankle joint.

C. Design principles

1) Effective torque generation: Secure anchoring of the actuator

In the previous section, we modeled the inflatable actuator as attached to each segment of the leg. If the actuator is loosely anchored to the body, the actuator inflates away from the ankle joint when it is pressurized (Fig. 3A). It results in little assistive torque being delivered to the joint and a reduction in the range of motion. Thus, in order to maximize the torque transmitted to the ankle joint, our design must ensure that the inflatable actuator is securely attached to the shank and the foot with the help of a custom-made boot. The lengths of the attachments to both the shank and foot segments are chosen by first centering the actuator at the ankle joint. Then the actuator is extended symmetrically along the foot and shin sides until it reaches 20mm before the first metatarsophalangeal joint. We also employ a lace tightening system to allow the boot to conform to and secure both the foot and shank tightly. Since the actuator is integrated on top of the tongue, the lacing system is implemented on both sides of the boot, as shown in Fig. 1B.

2) Minimize mechanical resistance of the boot

In addition to achieving secure anchoring, the rotational stiffness of the boot ought to be minimized in order to efficiently transmit the torque generated by the actuator to the foot. During ankle plantarflexion, the posterior side of the ankle contracts while its anterior side elongates. Our boot is designed to accommodate these biomechanical changes. Conventional boots are typically made of materials with high rotational stiffness, which inhibit boot deformation. The ExoBoot is custom-designed out of flexible fabric (see section II.D for details). This material choice is sufficient for posterior boot deformation. However, a section of inextensible woven material resists elongation on the anterior side. A cutout on the side of the boot from the outside of the fabric to the ankle joint is made as shown in Fig. 3B, so that the woven material does not impede ankle plantarflexion. With these modifications, we are able to achieve a boot that is securely attached to both the actuator and the foot without inhibiting the ankle's natural motion.

3) Assist plantarflexion in the sagittal plane while maintaining transparency for other ankle motions

Since the amount of the torque generated by the ExoBoot is significant, it is possible to induce undesirable ankle motion such as inversion and eversion during walking. Thus, it is critical to align the actuator in the sagittal plane and make the device transparent for other ankle motions. As shown in Fig. 1, the ExoBoot has a tightening system on both sides of a boot. The location of the actuator on top of the foot can be adjusted for each individual user separately with the tightening system. This custom adjustment allows the ExoBoot to assist sagittal plane motion and minimizes undesirable effects.

4) Human factors

To minimize the added distal mass and related increase of inertia of the leg, the ExoBoot is designed to be extremely light (255 g: body worn parts). A zipper is attached to the back to streamline donning and doffing. The average donning and doffing time of the boot is approximately 12 and 6 seconds, respectively. Finally, the open-toe design and lace tightening system enables the boot to accommodate foot sizes ranging from 250 mm to 290 mm in length (US 7.5-12.5).

D. Fabrication

The textile-based inflatable actuator must be airtight and resist high pressures up to 550 kPa (80 psi). An oversized thermoplastic polyurethane (TPU) bladder is chosen as the airtight component and is inserted into a smaller volume fabric enclosure, which reacts the stresses generated during inflation of the bladder. Flexible tubing (9.525 mm (3/8 inch) outer diameter) is glued in between two layers of TPU (Fiberglast, USA), which are then heat sealed together. The fabric enclosure is constructed with nylon (Seattle Fabrics, USA) such that it takes a cylindrical shape when fully inflated. The fabric enclosure has a triple stitched seam to resist the large stresses generated.

The components of the boot are shown in Fig. 3E. The boot body comprises two side parts and a tongue, each of which is constructed with two layers: Fabrifoam (Fabrifoam, USA) and urethane coated nylon (Seattle Fabrics, USA). The Fabrifoam layer provides high flexibility and a comfortable interface with the foot, while the woven nylon layer restricts extension of the boot away from the ankle. A lace tightening

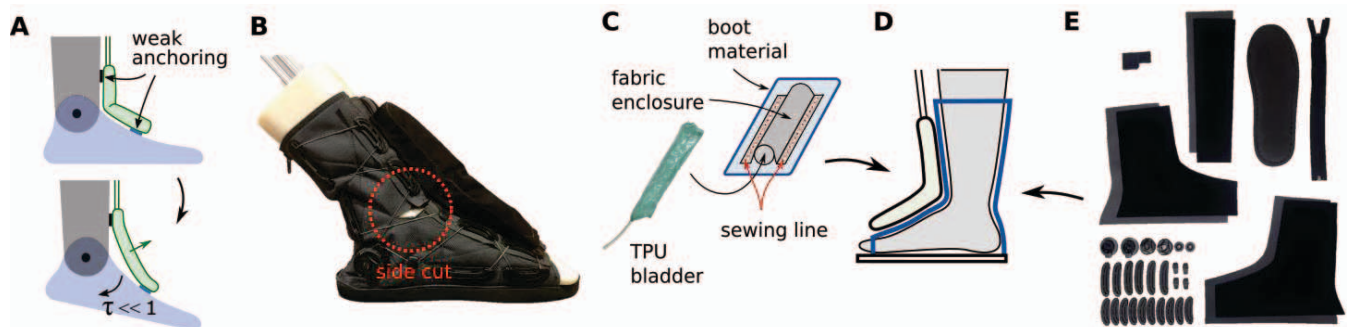


Figure 3 Design considerations **A**. Simplified diagram of the actuator-ankle system when the actuator is loosely anchored to the foot and the shin. The actuator exerted a small amount of torque to the foot, as it lifted away from the ankle upon pressurization. **B**. Side cuts on the boot prevent inextensible woven fabric from hindering ankle plantar flexion. **C**. Side sewing integration method. Both sides of the textile inflatable actuator are sewn to the boot. **D**. Cross sectional view of ExoBoot. The inflatable actuator is integrated to the custom-made boot. **E**. Components for the custom-made boot. The boot consists of the two sides of a body, a tongue, a sole, a lace tightening system, an IMU sensor case and a zipper.

system (Boa systems, USA) is sewn on both sides of the boot body and the tongue, and a zipper connects both sides at the back of the boot. The soft IMU case is made of two layers of FabriFoam and sewn to the boot between the toe and the lower edge of the actuator. Finally, the inflatable actuator is integrated to the boot. Both sides of the actuator are sewn to the tongue as shown in Fig. 3C.

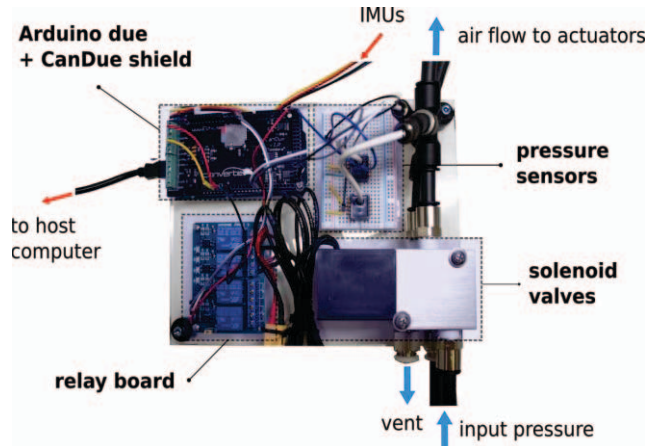


Figure 4 Overview of the control hardware. The flow from the compressor to the actuator is regulated by solenoid valves, which are controlled by an Arduino Due microcontroller receiving signals from foot-mounted IMUs. Sensors measure the pressure right after the valve outlet.

E. Actuation platform

The actuation platform is shown in Fig. 4. The pneumatic line source pressure comes from a compressor (D55146, DeWalt, USA), whose output pressure is regulated to the target steady-state pressure of the actuator using the built-in mechanical regulator. 3-way solenoid valves (320 12VDC, Humphrey, USA) control the air flow into the actuators and vent into the atmosphere. Pressure sensors (100PGAA5, Honeywell, USA) measure the pressure right after the valve outlet.

The valves are controlled using an Arduino Due microcontroller and are powered separately via a relay board (4 channel 5VDC relay module, Knacro, Hong Kong). A CAN shield (CANdue, EVT Motor Werks, USA) is used to communicate with the IMUs (MTi-1, XSens, USA) located on top of both feet using the CAN protocol. The control loop runs at 100Hz and data is recorded on a host computer using serial communication.

The required input pressure was expected to range from 276 kPa to 552 kPa (40-80 psi) in order to deliver 20 to 30 Nm peak torque, given the characterization work done for a similar actuation approach [17]. Recalling from section II.A that ideal inflation and deflation times are less than 250 and 150 ms respectively, large diameter tubing and high flow rate capacity valves that allow for flows in excess of 850 SLPM (Standard Liter Per Minute) were used because the required average inflation and deflation flow rates are expected to be on the order of 300 SLPM.

III. ACTUATION CHARACTERIZATION

We hypothesize that the pressure inside the TPU balloon is a main determinant of the torque that can be delivered by

the actuator. Indeed, the higher the pressure in the balloon, the higher the stress in the fabric enclosure wall and, consequently, the higher the torque generated.

We are mainly interested in how much torque the ExoBoot is able to exert to the foot and how fast it can be actuated. To characterize this, we first investigated the relation between pressure at the valve outlet and pressure at the actuator inlet, and we measured the torque generated by the ExoBoot at various supply pressures and ankle angles in static conditions.

A test fixture instrumented with a torque cell (Futek TFF350, USA) was developed to evaluate and characterize the actuator as shown in Fig. 5A. A simulated ankle joint was 3D printed to mimic the ankle joint movement. In this joint, the foot and the shank are connected with a plain bearing to minimize the friction between them. A stopper on the torque rig allowed for indexing of the ankle angle in 15 degrees increments. The bottom side of the boot and the torque rig were clamped so that the torque applied on the ankle joint can be measured through the shank.

Characterization was carried out at each static condition by applying a square wave pressure signal (0.25Hz, 50% duty cycle, 4 cycles total) to the actuator using our actuation platform while torque and pressure signals were captured at 1 kHz using a NI PCIe 6259 DAQ (National Instruments, USA) and Simulink (Mathworks, USA). This was repeated at each indexed joint angle θ_{ankle} , from 60 to 120 degrees in 15 degrees increments, and for input pressures p_i ranging from 138 kPa to 483 kPa (20-70 psi) by 69 kPa increments.

A. Pressure response

The ExoBoot system is designed to measure pressure near the valve outlet, because it is difficult to directly measure the pressure in the actuator during walking. Since there is about 1 m of tubing and connectors between the valve and the actuator, it is necessary to relate the valve outlet pressure to the actuator inlet pressure. To establish the relationship between them in static settings, we conducted a test to measure both values at the same time by adding a second pressure sensor near the actuator in static setting.

We investigated the pressure step response, as shown in Fig. 5B for a representative trial using 172 kPa (25 psi) input pressure and 90 degrees ankle angle. The pressure step response shows that there is a short transmission delay of the pressure curve between the valve outlet and the actuator, and that pressure spikes right after valve opening. The transmission delay is measured to be about 2-3 ms, which corresponds to the propagation of the pressure wave along the 1 m long tubing ($t = L/c = 2.9$ ms, with L the tubing length and c the speed of sound).

Regarding the large initial pressure spike, we hypothesize that it is a measurement artifact that does not reflect the true pressure. Indeed, the stagnation pressure p_{stag} measured by the sensor is given by

$$p_{stag} = p_{static} + \frac{1}{2}\rho v^2$$

where p_{static} is the static pressure in the tube, and v is the fluid velocity. When the pressure wave strikes the sensing element and stagnates, the dynamic pressure is converted to static

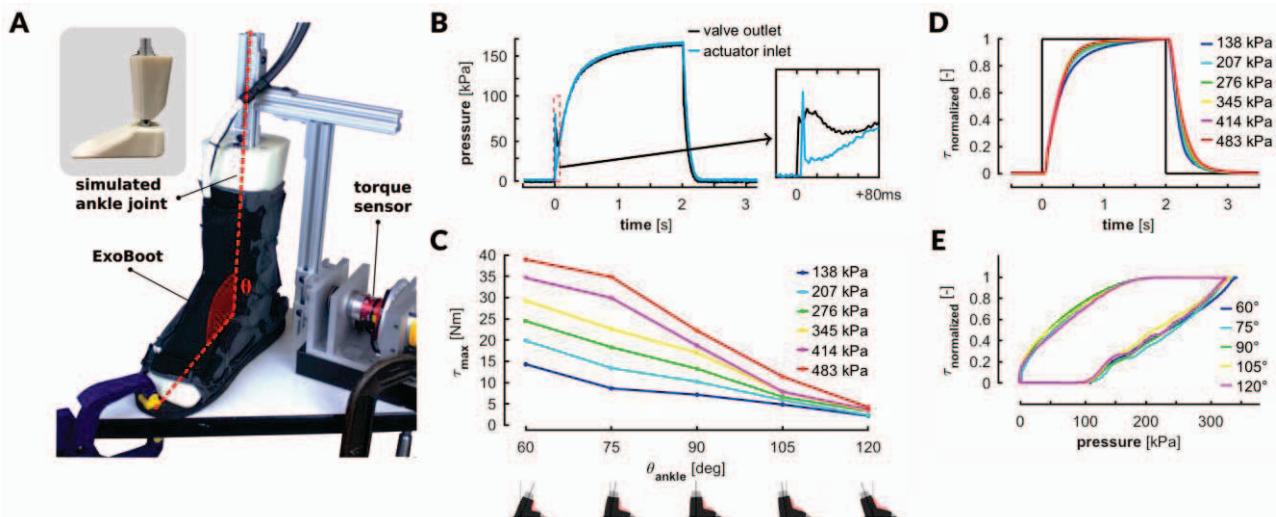


Figure 5 Actuator characterization on an instrumented rig for various angles and input pressures. **A.** The ExoBoot was mounted on a simulated ankle joint and torque was measured through the shank by clamping the bottom side of the boot and the torque rig. The shank angle was changed by 15 degrees increments so that the ankle angle ranged from 60 to 120 degrees. **B.** Pressure step response as a function of time, as measured at the valve outlet and the actuator inlet, for a given input pressure (172 kPa (25 psi)). The period of time right before and after valve opening is magnified on the right. **C.** Maximal steady-state torque for various angles and input pressures. **D.** Normalized torque response in function of time for a 60 degrees angle and various input pressures. The normalized pressure command is shown in black. **E.** Normalized torque response in function of measured pressure for a 345 kPa (50 psi) input pressure, for various angles.

pressure. It can be observed that this pressure spike lasts a very short amount of time at the actuator inlet, but it lasts longer at the valve outlet. This might be explained by the fact that the resistance between the measurement point and the lowest pressure point (the balloon) is bigger in the latter case.

We can estimate the pressure in the actuator using the one measured at the valve outlet by considering the aforementioned transmission delay and the measurement error. The estimated pressure seems to fit well the response of a first order linear system ($R^2 = 0.9908$).

B. Torque Response

At steady state, the soft inflatable robotic boot generated a maximum torque of 39 Nm while pressurized at 483 kPa (70 psi) for a joint angle set at 60 degrees, as shown in Fig. 5C.

Several observations can be made about the dynamics of the normalized torque response shown in Fig. 5D. First, the torque response seems to match that of a first order linear system ($R^2 = 0.9985$). Second, there is a delay of approximately 40 ms between the valve opening (which takes 15 ms) and the onset of torque.

The delay between pressure onset and torque onset was investigated by analyzing high speed video recordings (iPhone 6, 240 FPS). There are three delay components: (1) a pressure transmission delay (2-3 ms) between the valve outlet and the actuator (see section III.A for details), (2) a balloon inflation delay (20-30 ms), (3) a textile component deformation delay (5-10 ms). When we supply compressed air to the deflated inflatable actuator, the balloon volume increases first for 20-30 ms until it is constrained by the fabric enclosure. Then the textile component of the ExoBoot between the actuator and the foot compressed for 5-10 ms before the actuator starts applying force to the foot due to low stiffness of the FabriFoam layer. By looking at each frame of the highspeed video, we were able to observe that the

measured torque is about 0 Nm while the actuator is being inflated and the textile component of the ExoBoot is being deformed.

The hysteric behavior of normalized torque compared to the measured pressure highlights the different dynamics between inflation and deflation, as well as the transient behavior occurring right after the step commanded pressure, as shown in Fig. 5E. Indeed, fast and transient pressure jumps during which the torque is kept constant can be observed right after valve opening and closing. More importantly, the relationship between normalized torque and pressure is independent of the angle at any time as shown in Fig. 7C.

IV. CONTROL

An open loop pressure controller triggers the inflation and deflation of the boot as a function of the phase of the gait cycle. Phase in the gait cycle was measured using the embedded IMU. A simple strategy consisting of tuning the opening and closing times of a solenoid valve, as well as utilizing a constant pressure source, was chosen in order to leverage the observations of step responses. Based on section II.A, target torque timings are 30% GC for onset, 50% GC for peak and 65% GC for off timing.

An accurate measure of gait cycle percentage is required to time the assistance correctly. As with previous studies, the first peak in the sagittal angular velocity of the foot is detected as this event was reported to correspond to 4% GC [26]. Typical evolution of the ankle angular velocity is shown in Fig. 6, together with the aforementioned gait event. The gait percentage can then be computed based on the average frequency of the two previous steps, this approach being well suited for treadmill environment where the stride frequency variability is limited.

Given our desired timings of assistive torque, the valve opening and closing timings were set after considering the

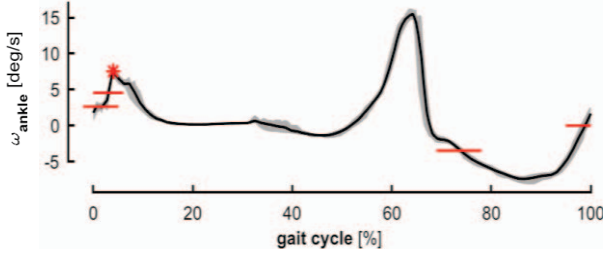


Figure 6 Gait segmentation algorithm. The ankle angular velocity is shown as a function of gait cycle for a subject walking on treadmill at 1.3 m/s. A set of thresholds allows to detect the gait event shown as a red star, which corresponds to 4% GC approximately [26].

aforementioned 3% GC delay between pressure and torque onset. After slight tuning based on user feedback, T_{ON} and T_{OFF} were chosen to be 30% and 55% GC so that the torque would onset at 33% GC and peak before 58%. The torque off timing would ideally be 65% GC but given the limitation of a slow deflation time of the large volume actuators, it is expected to happen later than the desired value, close to 80% GC.

The input pressure was set as high as possible (586 kPa) to deliver enough assistance without damaging the actuator.

V. DYNAMIC TORQUE ESTIMATION

Experimental characterization was performed to estimate the assistive torque generated by the ExoBoot during walking. The soft nature of the ExoBoot means that no traditional sensor could directly measure the assistance delivered by the actuator precisely. Even though pressure inside the balloon is the primary variable that is controlled, the torque profile can be estimated by leveraging results from the previously described characterization of the boot on the instrumented rig. An estimation method is then proposed to predict the dynamic torque response based on static characterization data.

The main difference compared to the system characterization done before is that the ankle angle changes during walking. If the assistive torque generated by the ExoBoot is independent of ankle angle time derivatives (angular velocity and acceleration), i.e. the behavior of the actuator is similar in both static and dynamic settings, then the assistive torque can be estimated using a map of torque with respect to time and ankle angle, as measured in the static experiments.

During inflation (between T_{ON} and T_{OFF}), it seems reasonable to assume that ankle angle time derivatives have limited effects on the torque profile because the ankle rotation is very limited, as shown in Fig. 7A. However, during deflation, the reliability of the torque estimation during this phase is likely limited because the ankle angle changes more rapidly. Nevertheless, this doesn't affect the estimated peak torque, which is a critical metric to predict the net metabolic reduction for wearable robots [6].

Based on these assumptions, a map of torque, which is a function of the time after the valve has opened and the ankle angle at this time $\theta(t)$, is then found for each input pressure p_i , by interpolating the torque responses at any time t for

angles comprised between 60 and 120 degrees. This map is shown in Fig. 7C for $p_i = 414$ kPa (60 psi).

Given the typical ankle angle profile shown in Fig. 7A and assuming a typical gait cycle duration of 1.2 s, an estimation of the torque profile can be obtained, as shown in Fig. 7C. Delays of 40 ms between pressure and torque onset and between pressure and torque off timing were considered, as characterized in section III.

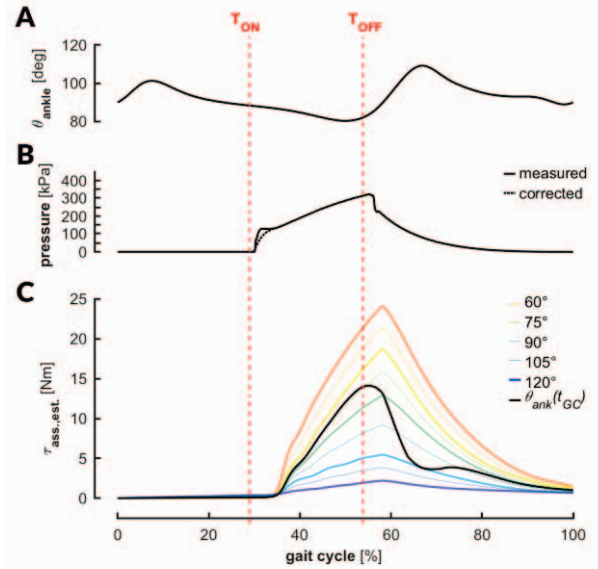


Figure 7 Actuation profile and estimation of the assistive torque. **A.** The ankle angle from walking at 1.25 m/s measured by a motion capture system in our previous study. **B.** The expected pressure profile as a function of gait cycle. **C.** The torque map and the estimated torque profile. Static torque responses for various ankle angles as a function of time for inflation (left of vertical dashed line) and deflation (right of vertical dashed line) of the actuator with an input pressure of 414 kPa (60 psi) are shown. The black line depicts the estimated torque profile for a typical ankle angle trajectory and gait cycle duration. This torque map, computed for each input pressures, can be used to estimate the assistive torque profile.

VI. DEVICE PERFORMANCE EVALUATION

The performance of the device was evaluated by a healthy individual wearing a pair of ExoBoots while walking on a treadmill at 1.3 m/s for 1 min while pressure signals were recorded. The experimental setup is shown in Fig. 8A. The source pressure was varied using the pressure regulator on the compressor. The assistive torque shown in Fig. 8C was estimated knowing the input pressure and the typical evolution of the ankle angle, as well as results obtained during characterization of the actuator in static conditions, the procedure being detailed in section V.

The control hardware and algorithm consistently delivered an assistive pressure profile with low step-to-step variability, as shown in Fig. 8B. The balloon pressure reached approximately 75% of the line pressure, as seen during characterization. The average onset, peak and off timings of the measured pressure profile were found to be $31 \pm 0.4\%$ GC, $55 \pm 0.5\%$ GC and $79.1 \pm 3.8\%$ GC respectively.

The estimated torque profile timings are estimated to be 34% GC for the onset, 56% GC for the peak and 80% GC for

the off timing. The maximal peak torque value that could be reached is estimated to be 23 Nm when using a 586 kPa (85 psi) supply pressure.

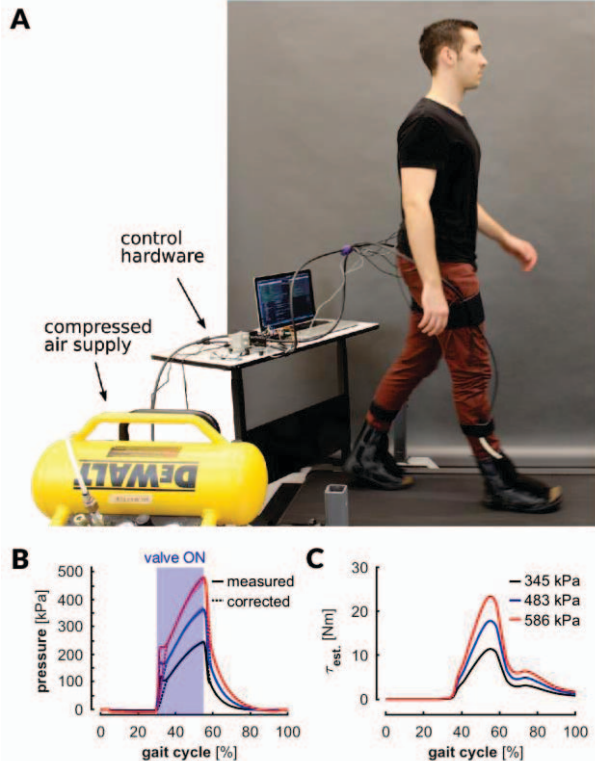


Figure 8 Evaluation of the device performance during treadmill walking. **A.** Overview of the treadmill walking test setup. **B.** Measured pressure profile as a function of the gait cycle variable estimated by our algorithm during walking at 1.3 m/s for various input pressures. **C.** Estimated assistive torque profile as a function of gait cycle, assuming a typical ankle angle walking profile.

VII. CONCLUSION AND FUTURE WORK

In conclusion, this work presents a preliminary design and evaluation of the ExoBoot, a soft inflatable robotic boot for assisting ankle plantarflexion. A textile-based inflatable actuator sewn on a soft textile boot generates assistive torque using pneumatic pressure. The boot is designed to be soft and lightweight for minimizing rotational stiffness and added distal mass.

Actuation characterization and evaluation of the device on the treadmill show it can deliver controlled assistance during walking. The ExoBoot exerted a maximum torque of 39 Nm in static testing with 483 kPa (70 psi) supply pressure at 60 degrees ankle angle. During the walking test, pressure in the actuator reaches 75% of supply pressure at the peak of active assistance, and maximum torque applied on an ankle was estimated as 23 Nm. Referring to previous work with soft assistive devices for gait augmentation [6], we hypothesize that the tethered ExoBoot can have a positive effect at reducing the metabolic cost of walking.

Future work will include design optimization of the actuator and implementation of advanced control strategies. It is shown from the static torque measurement that the ExoBoot exerts maximum torques at low ankle angle, around

60 degrees. We are planning to explore different geometries of the inflatable actuator to optimize torque characteristic with respect to angle, since the ankle angle during our target actuation timing is around 90 degrees. Also, this version of the ExoBoot consumes about 0.35 liter of pressurized air supply per boot every second, which leads to slow inflation and deflation time with our existing air supply. One approach to address this problem may be to reduce actuator volume by employing segmented inflatable actuator and rigid components for interfacing between the actuator and the boot [16].

Future iterations will employ proportional air valves and additional IMUs for increased control of the assistance. This will allow us to estimate instantaneous ankle angles and enable us to prescribe desired pressure trajectories for the ExoBoot. Once we can control ankle angle and pressure, torque profile control can be investigated using the ExoBoot. The effectiveness of assistance will be quantified by measuring the wearer's metabolic cost reduction.

We have identified limitations of our work and plan to address them in a future study. We did not quantitatively measure the effect of actuation for different ankle motions other than plantarflexion and this should be further characterized. The robustness of the actuator has not been determined and a cycle test will be performed. Lastly, we plan to test the device at various walking speeds and explore effects on wearer energetics.

ACKNOWLEDGMENT

The authors would like to thank Dorothy Orzel for her assistance with apparel design skills.

REFERENCES

- [1] J. Bae *et al.*, "A soft exosuit for patients with stroke: Feasibility study with a mobile off-board actuation unit," *IEEE Int. Conf. Rehabil. Robot.*, vol. 2015–Sept, pp. 131–138, 2015.
- [2] L. N. Awad *et al.*, "A soft robotic exosuit improves walking after stroke," *Sci. Transl. Med.*, vol. In Press, no. July, 2017.
- [3] P. Malcolm, W. Derave, S. Galle, and D. De Clercq, "A Simple Exoskeleton That Assists Plantarflexion Can Reduce the Metabolic Cost of Human Walking," *PLoS One*, vol. 8, no. 2, pp. 1–7, 2013.
- [4] L. M. Mooney *et al.*, "Autonomous exoskeleton reduces metabolic cost of human walking during load carriage," *J. Neuroeng. Rehabil.*, vol. 11, no. 1, p. 80, 2014.
- [5] S. H. Collins, M. Bruce Wiggin, and G. S. Sawicki, "Reducing the energy cost of human walking using an unpowered exoskeleton," *Nature*, vol. 522, no. 7555, pp. 212–215, 2015.
- [6] B. T. Quinlivan *et al.*, "Assistance magnitude versus metabolic cost reductions for a tethered multiarticular soft exosuit," *Sci. Robot.*, vol. 2, no. 2, p. eaah4416, 2017.
- [7] H. Kazerooni and R. Steger, "The Berkeley Lower Extremity Exoskeletons," *ASME J. Dyn. Syst. Meas. Control*, vol. 128, no. 1, pp. 14–25, 2006.
- [8] C. J. Walsh, K. Endo, and H. Herr, "A Quasi-Passive Leg Exoskeleton for Load-Carrying Augmentation," *Int. J. Humanoid Robot.*, vol. 4, no. 3, pp. 487–506, 2007.
- [9] S. Rossi, A. Colazza, M. Petrarca, E. Castelli, and P. Cappa, "Feasibility Study of a Wearable Exoskeleton for Children: Is the Gait Altered by Adding Masses on Lower Limbs?," *PLoS One*, vol. 8, no. 9, pp. 1–9, 2013.
- [10] R. C. Browning, J. R. Modica, R. Kram, and A. Goswami, "The effects of adding mass to the legs on the energetics and biomechanics of walking," *Med. Sci. Sports Exerc.*, vol. 39, no. 3, pp. 515–525, 2007.

- [11] G. S. Sawicki and D. P. Ferris, "A pneumatically powered knee-ankle-foot orthosis (KAFO) with myoelectric activation and inhibition," *J. Neuroeng. Rehabil.*, vol. 6, no. 1, pp. 1–16, 2009.
- [12] F. A. Panizzolo *et al.*, "A biologically-inspired multi-joint soft exosuit that can reduce the energy cost of loaded walking," *J. Neuroeng. Rehabil.*, vol. 13, no. 1, p. 43, 2016.
- [13] M. Wehner *et al.*, "A lightweight soft exosuit for gait assistance," *Proc. - IEEE Int. Conf. Robot. Autom.*, pp. 3362–3369, 2013.
- [14] Y. L. Park *et al.*, "Design and control of a bio-inspired soft wearable robotic device for ankle-foot rehabilitation," *Bioinspiration and Biomimetics*, vol. 9, no. 1, 2014.
- [15] P. Polygerinos, Z. Wang, K. C. Galloway, R. J. Wood, and C. J. Walsh, "Soft robotic glove for combined assistance and at-home rehabilitation," *Rob. Auton. Syst.*, vol. 73, pp. 135–143, 2015.
- [16] S. Sovero, N. Talele, C. Smith, N. Cox, T. Swift, and K. Byl, "Initial data and theory for a high specific-power ankle exoskeleton device," *Proc. IEEE Int. Symp. on Experimental Robotics (ISER)*, pp. 355–364, 2016.
- [17] S. Sridar *et al.*, "Development of a Soft-Inflatable Exosuit for Knee Rehabilitation," *Proc. IEEE/RSJ Inter. Conf. Intel. Robot. Sys. (IROS)*, pp. 3722–3727, 2017.
- [18] Y. Kadowaki, T. Noritsugu, M. Takaiwa, D. Sasaki, and M. Kato, "Development of soft power-assist glove and control based on human intent," *J. Robot. Mechatronics*, vol. 23, no. 2, pp. 281–291, 2011.
- [19] P. Polygerinos, K. C. Galloway, S. Sanan, M. Herman, and C. J. Walsh, "EMG controlled soft robotic glove for assistance during activities of daily living," *IEEE Int. Conf. Rehabil. Robot.*, vol. 2015–Sept, pp. 55–60, 2015.
- [20] C. T. O'Neill, N. S. Phipps, L. Cappello, S. Paganoni, and C. J. Walsh, "A soft wearable robot for the shoulder: Design, characterization, and preliminary testing," *2017 Int. Conf. Rehabil. Robot.*, vol. 2129, pp. 1672–1678, 2017.
- [21] D. J. Farris and G. S. Sawicki, "The mechanics and energetics of human walking and running: a joint level perspective," *J. R. Soc. Interface*, vol. 9, no. 66, pp. 110–118, 2012.
- [22] A. T. Asbeck, S. M. M. De Rossi, I. Galiana, Y. Ding, S. Member, and C. J. Walsh, "Stronger , Smarter , Softer : Next Generation Wearable Robots," *IEEE Robot. Autom. Mag.*, vol. 21, no. 4, pp. 22–33, 2014.
- [23] S. Galle, P. Malcolm, S. H. Collins, and D. De Clercq, "Reducing the metabolic cost of walking with an ankle exoskeleton: interaction between actuation timing and power," *J. Neuroeng. Rehabil.*, vol. 14, no. 1, pp. 1–16, 2017.
- [24] J. Zhang *et al.*, "Human-in-the-loop optimization of exoskeleton assistance during walking," *Science*, vol. 356, no. 6344, pp. 1280–1283, 2017.
- [25] M. D. Latt, H. B. Menz, V. S. Fung, and S. R. Lord, "Walking speed, cadence and step length are selected to optimize the stability of head and pelvis accelerations," *Exp. Brain Res.*, vol. 184, no. 2, pp. 201–209, 2008.
- [26] Y. Ding *et al.*, "Effect of timing of hip extension assistance during loaded walking with a soft exosuit," *J. Neuroeng. Rehabil.*, vol. 13, no. 1, pp. 1–10, 2016.